Research Paper
Computational Methods for Differential Equations
http://cmde.tabrizu.ac.ir
Vol. 14, No. 2, 2026, pp. 903-913
DOI:10.22034/cmde.2025.64267.2901

Stability analysis of SAIR mathematical model with general incidence rates and temporary immunity

Nemat Nyamoradi[1,*], **Karam Allali**[2], **and Bashir Ahmad**[3]

[1]Department of Mathematics, Faculty of Sciences, Razi University, 67149 Kermanshah, Iran.

[2]Laboratory of Mathematics, Computer Science and Applications, Faculty of Sciences and Technologies, University Hassan II of Casablanca, PO Box 146, Mohammedia, Morocco.

[3]Nonlinear Analysis and Applied Mathematics (NAAM)-Research Group, Department of Mathematics, Faculty of Science, King Abdulaziz University, P.O. Box 80203, Jeddah 21589, Saudi Arabia.

Abstract

This paper studies the dynamics of a SAIR mathematical model that describes the interaction among susceptible, asymptomatic, symptomatic, and recovered individuals. Two general incidence functions describing the infection caused by the asymptomatic and symptomatic individuals are introduced. We also take into account a temporary immunity, that is, a proportion of the recovered individuals becomes susceptible again. The basic reproduction number R_0 depends on the general incidence functions. The local and global asymptotical stability for each equilibrium will depend on the basic reproduction number R_0. In precise terms, the disease-free equilibrium is locally and globally asymptotically stable when $R_0 < 1$, while the endemic equilibrium is locally and globally asymptotic stable when $R_0 > 1$. The numerical simulation is performed for different incidence rate cases, such as bilinear, Beddington-DeAngelis, Crowley-Martin, and non-monotonic incidence rate functions. The simulation results are found to agree with the theoretical endings.

Keywords. SAIR mathematical model, Stability, Basic reproduction number, Periodic orbit.

2010 Mathematics Subject Classification. 92D30, 34D20, 34D23.

1. Introduction

The coronavirus (COVID-19) pandemic severely affected the human activities and restricted the daily life of the people to social isolation, wearing of masks, and so on. All the health organizations and the WHO made a desperate effort to control its rapid spread by organizing several seminars and workshops. The tool of mathematical modelling played an effective and important role in the study of epidemic diseases such as malaria, smallpox, the plague epidemic in India, HIV, etc. Kermack and McKendrick [20] introduced the first complete mathematical model in epidemiology to study a plague epidemic in India in 1906 by using the ideas presented in [17, 30]. The duration of the disease is an important factor to be taken into account, as a person who remains infected for many days can potentially infect a large community of individuals. A virus like COVID-19 is more likely to be contagion, but an infected person can transmit it to many people. One of the important mathematical models in epidemiology is SIR, which consists of three groups: (S) susceptible, (I) infected, and (R) recovered. Models such as SIS, SEIR, and SIRC are variants of the SIR model; for details, see [1–3, 8, 11, 19, 22, 23, 28, 29, 32] and the references therein.

It is well known that infections such as COVID-19 experience many asymptomatic cases during its spread. The main issue is that the easily infect any susceptible person. Additionally, this asymptomatic period can be a longer one without exposing the real condition of the asymptomatic virus carrier. With the high cost of COVID-19 virus clinical tests, the asymptomatic individuals remain an important infection transmission factor. Therefore, many mathematical

Received: 30 October 2024; Accepted: 17 February 2025.
∗ Corresponding author. Email: neamat80@yahoo.com, nyamoradi@razi.ac.ir.

models have taken into consideration the asymptomatic compartment to model COVID-19; for example, see the texts [7, 12, 35].

Therefore, we study the following SAIR model (S (the densities of the population that are susceptible), A (asymptomatic), I (infected) and R (recovered with temporary immunity) with general incidence rates as follows:

$$\begin{cases} \frac{dS}{dt} = \lambda - \mathcal{F}(S,A) - \mathcal{G}(S,I) - \mu S + \tau R, \\ \frac{dA}{dt} = \mathcal{F}(S,A) + \mathcal{G}(S,I) - \mu A - \phi A, \\ \frac{dI}{dt} = \phi A - \mu I - \gamma I, \\ \frac{dR}{dt} = \gamma I - \mu R - \tau R, \end{cases} \tag{1.1}$$

where $\mathcal{F}(S,A)$ denotes the general incidence rates of contagions produced by asymptomatic persons, $\mathcal{G}(S,I)$ represents general incidence rates of contagions produced by an infected person, and λ is the recruitment rate in the first group, μ denotes the natural plus disease death rate in each group, γ is the recovery rate, ϕ is the pollution rate, and τ is the rate at which the recovered population from infection again joins the susceptible class. Also, the total population size N is the sum of the sizes of these four classes: $N(t) = S(t) + A(t) + I(t) + R(t)$.

It is practically impossible to carry out virus clinical tests on the entire population. Therefore, the asymptomatic individuals remain free to move within the safe population. This is why we have chosen a general infection force of the form $\mathcal{F}(S,A) + \mathcal{G}(S,I)$, which takes into account the infection caused by both asymptomatic and infected individuals. Moreover, the general infection rate will give us a broader view of the infection spread as demonstrated in the numerical simulation section.

Many authors studied the mathematical model of COVID-19 with a general incidence rate. For instance, the stability of the SIR COVID-19 infection model with a general incidence rate was studied in [1]. In [22, 23], the authors considered a multi-strain SEIR COVID-19 infection with general incidence rates and studied the global stability of each strain dynamics. Recently, in [31], the authors studied a fractional order differential equation model of SARS-CoV-2 infection.

The flow diagram representing our epidemiological case is illustrated in Figure 1. Here, the infected individuals are subdivided into two classes; the first represents the asymptomatic infected population, while the second one presents the symptomatic individuals. Both the subclasses may infect any susceptible individual. For this reason, the asymptomatic compartment is added to many epidemiological mathematical models, which are known as SAIR mathematical models [14, 24]. For instance, in [15], the authors explored this new compartment to investigate its impact on the dengue disease model. In a recent work [4], an SAIR mathematical model describing the COVID-19 pandemic was considered to study the effect of lockdown on reducing the infection severity. In a related work [27], the authors investigated the different conditions in the SAIR mathematical model to eradicate the malady. The articles [4, 27] introduced the bilinear incidence function to describe the infection rate. In this paper, we assume both the infection rates caused by the asymptomatic and symptomatic individuals in their general form. Moreover, we take into account a temporary immunity for the recovered persons, which means that a proportion of the recovered becomes again susceptible.

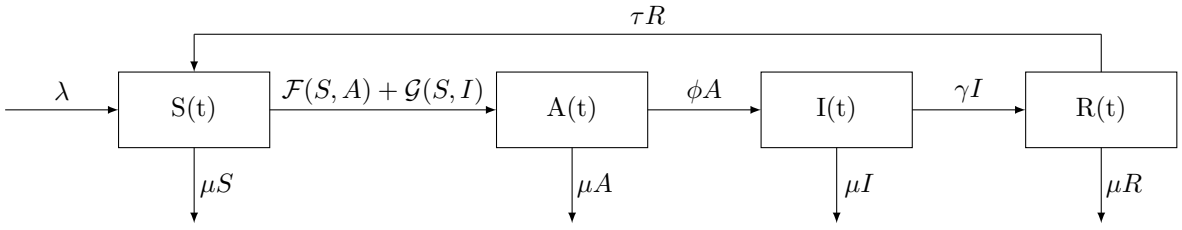

FIGURE 1. The flowchart of SAIR infection model.

The nonlinear incidence functions $\mathcal{F}(S,A), \mathcal{G}(S,I) \in C^1(\mathbb{R}^+ \times \mathbb{R}^+, \mathbb{R}^+)$ satisfy the following conditions:

$$\begin{cases} (H1) & \forall S,A,I>0, \quad \mathcal{F}(S,A),\mathcal{G}(S,I)>0, \\ (H2) & \forall S,A,I\geq 0, \quad \mathcal{F}(S,0)=\mathcal{F}(0,A)=0, \quad \mathcal{G}(s,0)=\mathcal{G}(0,I)=0, \\ (H3) & \forall S\geq 0, A,I>0 \quad \frac{\partial \mathcal{F}(S,A)}{\partial S} \text{ and } \frac{\partial \mathcal{G}(S,I)}{\partial S} \text{ are bounded and } \frac{\partial \mathcal{F}(S,A)}{\partial S}, \frac{\partial \mathcal{G}(S,I)}{\partial S}>0, \\ (H4) & \forall S,A,I\geq 0, \frac{\partial \mathcal{F}(S,A)}{\partial A}>0, \frac{\partial \mathcal{G}(S,I)}{\partial I}<0, \frac{\partial \mathcal{F}(S,A)}{\partial A}<\mu+\phi, \frac{\partial \mathcal{G}(S,I)}{\partial I}<-\frac{\gamma\tau}{\mu+\tau}, \\ (H5) & \forall S,A,I\geq 0, \quad A\frac{\partial \mathcal{F}(S,A)}{\partial A}-\mathcal{F}(S,A)<0, \ I\frac{\partial \mathcal{G}(S,I)}{\partial I}-\mathcal{G}(S,I)<0. \end{cases}$$

The incidence rate $\mathcal{F}(S,A)$ depends on the densities of susceptible and asymptomatic individuals and may be of the form $\frac{\theta SA}{S+A}$, $\frac{\beta SA}{1+\sigma A}$, and $\frac{\theta SA}{1+\varrho_1 S+\varrho_2 A}$. The incidence rate $\mathcal{G}(S,I)$ is dependent on the densities of susceptible and infected individuals and may be of the form $\frac{\theta S}{1+\varrho I}$, $\frac{\theta S}{1+\varrho_1 S+\varrho_2 I}$, and $\frac{\theta S}{1+\varrho_1 S+\varrho_2 I+\varrho_1\varrho_2 SI}$. For more details on $\mathcal{F},\mathcal{G}$, we refer the readers to [6, 9, 10, 13, 25, 26, 36, 37] and the references therein.

The paper is organized as follows: in the next section, we will perform the stability analysis of our epidemiological model. Section 3 is devoted to the numerical simulations of our SAIR model. The last section contains the concluding remarks.

2. Stability analysis

Lemma 2.1. *For all non-negative initial data, the solution $(S(t),A(t),I(t),R(t))$ of system (1.1) exists non-negative for all $t>0$ and remains bounded.*

Proof. The existence and uniqueness of the solution of system (1.1) follow form the standard arguments [16]. The positivity of solutions can be shown by using the method employed in [[21], Lemma 3.1]. Now, we claim that the solution of (1.1) remains bounded. To this end, let $N(t)=S(t)+A(t)+I(t)+R(t)$ so that $\dot{N}=\dot{S}+\dot{A}+\dot{I}+\dot{R}=\lambda-\mu N$. In consequence, we get

$$N(t)=\frac{\lambda}{\mu}+(N(0)-\frac{\lambda}{\mu}e^{-\mu t}).$$

Hence, for all $t\geq 0$, we have $N(t)\leq \frac{\lambda}{\mu}+N(0)$. Obviously, N is bounded, and so $S,\ A,\ I$, and R are bounded. □

We now discuss the basic reproduction number and equilibrium points of the system (1.1).

We now obtain the equilibrium points of (2) by calculating solutions of the following system:

$$\begin{cases} \lambda-\mathcal{F}(S,A)-\mathcal{G}(S,I)-\mu S+\tau R=0, \\ \mathcal{F}(S,A)+\mathcal{G}(S,I)-\mu A-\phi A=0, \\ \phi A-\mu I-\gamma I=0, \\ \gamma I-\mu R-\tau R=0. \end{cases} \tag{2.1}$$

To find disease-free equilibrium, I should be zero in (2.1), and so the system (1.1) has a unique disease-free equilibrium $\Theta_0=\left(\frac{\lambda}{\mu},0,0,0\right)$. Now, we find the basic reproduction number R_0 of system (1.1) as found in [33]. By the Jacobian of (1.1) around Θ_0, set

$$\bar{F}=\begin{pmatrix} \frac{\partial \mathcal{F}}{\partial A}\left(\frac{\lambda}{\mu},0\right) & \frac{\partial \mathcal{G}}{\partial I}\left(\frac{\lambda}{\mu},0\right) & 0 \\ 0 & 0 & 0 \\ 0 & 0 & 0 \end{pmatrix}, \qquad \bar{V}=\begin{pmatrix} \mu+\phi & 0 & 0 \\ -\phi & \mu+\gamma & 0 \\ 0 & -\gamma & \mu+\tau \end{pmatrix}. \tag{2.2}$$

So, by calculating $\bar{F}\bar{V}^{-1}$ and its spectral radius, we find R_0 given by

$$R_0=\frac{1}{\mu+\phi}\left[\frac{\partial \mathcal{F}(\frac{\lambda}{\mu},0)}{\partial A}+\frac{\phi}{\mu+\gamma}\frac{\partial \mathcal{G}(\frac{\lambda}{\mu},0)}{\partial I}\right]. \tag{2.3}$$

Theorem 2.2. *(1) If $R_0\leq 1$, then system (1.1) has a unique disease-free equilibrium $\Theta_0=(\frac{\lambda}{\mu},0,0,0)$.*

(2) If $R_0>1$, then system (1.1) has a unique endemic equilibrium $\Theta^*=(S^*,A^*,I^*,R^*)$.

Proof. We obtain the equilibrium points of (1.1) by solving the following system:

$$\begin{cases} \frac{dS}{dt} = \lambda - \mathcal{F}(S,A) - \mathcal{G}(S,I) - \mu S + \tau R = 0, \\ \frac{dA}{dt} = \mathcal{F}(S,A) + \mathcal{G}(S,I) - (\mu+\phi)A = 0, \\ \frac{dI}{dt} = \phi A - (\mu+\gamma)I = 0, \\ \frac{dR}{dt} = \gamma I - (\mu+\tau)R = 0. \end{cases} \tag{2.4}$$

Hence, we have

$$I = \frac{\phi}{\mu+\gamma}A, \quad R = \frac{\gamma}{\mu+\tau}I, \tag{2.5}$$

$$S = \frac{\lambda(\mu+\gamma)(\mu+\tau) - \zeta_1 A}{\zeta_2}, \tag{2.6}$$

where $\zeta_1 = (\mu+\phi)(\mu+\gamma)(\mu+\tau) - \tau\gamma\phi > 0$ and $\zeta_2 = \mu(\mu+\gamma)(\mu+\tau) > 0$. Note that $S \geq 0$ if and only if $E \leq \frac{\lambda(\mu+\gamma)(\mu+\tau)}{\zeta_1}$. From the second equation of (2.4), we get

$$\mathcal{F}\left(\frac{\lambda(\mu+\gamma)(\mu+\tau) - \zeta_1 A}{\zeta_2}, A\right) + \mathcal{G}\left(\frac{\lambda(\mu+\gamma)(\mu+\tau) - \zeta_1 A}{\zeta_2}, \frac{\phi}{\mu+\gamma}E\right) - (\mu+\phi)A = 0.$$

Define

$$\mathcal{H}(A) := \mathcal{F}\left(\frac{\lambda(\mu+\gamma)(\mu+\tau) - \zeta_1 A}{\zeta_2}, A\right) + \mathcal{G}\left(\frac{\lambda(\mu+\gamma)(\mu+\tau) - \zeta_1 A}{\zeta_2}, \frac{\phi}{\mu+\gamma}A\right) - (\mu+\phi)A.$$

By (H2), clearly, $H(0) = 0$,

$$\begin{aligned} \mathcal{H}\left(\frac{\lambda(\mu+\gamma)(\mu+\tau)}{\zeta_1}\right) &= \mathcal{F}\left(0, \frac{\lambda(\mu+\gamma)(\mu+\tau)}{\zeta_1}\right) + \mathcal{G}\left(0, \frac{\phi}{\mu+\gamma}\cdot\frac{\lambda(\mu+\gamma)(\mu+\tau)}{\zeta_1}\right) - (\mu+\phi)\frac{\lambda(\mu+\gamma)(\mu+\tau)}{\zeta_1} \\ &= -\frac{\lambda(\mu+\gamma)(\mu+\tau)(\mu+\phi)}{\zeta_1} < 0. \end{aligned}$$

Also, by relation $\frac{\partial \mathcal{G}}{\partial A} = \frac{\partial \mathcal{G}}{\partial I}\frac{\partial I}{\partial A} = \frac{\phi}{\mu+\gamma}\frac{\partial \mathcal{G}}{\partial I}$, we get

$$\begin{aligned} \mathcal{H}'(0) &= \frac{\partial \mathcal{F}(\frac{\lambda}{\mu}, 0)}{\partial A} + \frac{\partial \mathcal{G}(\frac{\lambda}{\mu}, 0)}{\partial A} \\ &= \frac{\partial \mathcal{F}(\frac{\lambda}{\mu}, 0)}{\partial A} + \frac{\phi}{\mu+\gamma}\frac{\partial \mathcal{G}(\frac{\lambda}{\mu}, 0)}{\partial I} \\ &= (\mu+\phi)(R_0 - 1). \end{aligned}$$

This yields

$$A^* \in \left(0, \frac{\lambda(\mu+\gamma)(\mu+\tau)}{\zeta_1}\right], \tag{2.7}$$

such that $\mathcal{H}(E^*) = 0$ if $R_0 > 1$, which, in turn, implies that (1.1) admits an infection equilibrium $\Theta^* = (S^*, A^*, I^*, R^*) \in (\mathbb{R}^+)^4$. We now show that the infection equilibrium is unique. To this end, by the second equation of (2.4), we have

$$(\mu+\phi) = \frac{\mathcal{F}(S^*, A^*) + \mathcal{G}(S^*, I^*)}{A^*}.$$

Using $I^* = \frac{\phi}{\mu+\gamma}A^*$, (H3) and (H5), we get

$$\begin{aligned}
\mathcal{H}^{'}(A^*) &= -\frac{\zeta_1}{\zeta_2}\frac{\partial \mathcal{F}(S^*,A^*)}{\partial S} + \frac{\partial \mathcal{F}(S^*,A^*)}{\partial A} \\
&\quad - \frac{\zeta_1}{\zeta_2}\frac{\partial \mathcal{G}(S^*,\frac{\phi}{\mu+\gamma}A^*)}{\partial S} + \frac{\phi}{\mu+\gamma}\frac{\partial \mathcal{F}(S^*,\frac{\phi}{\mu+\gamma}A^*)}{\partial I} - (\mu+\phi) \\
&= -\frac{\zeta_1}{\zeta_2}\frac{\partial \mathcal{F}(S^*,A^*)}{\partial S} + \frac{\partial \mathcal{F}(S^*,A^*)}{\partial A} \\
&\quad - \frac{\zeta_1}{\zeta_2}\frac{\partial \mathcal{G}(S^*,\frac{\phi}{\mu+\gamma}A^*)}{\partial S} + \frac{\phi}{\mu+\gamma}\frac{\partial \mathcal{F}(S^*,\frac{\phi}{\mu+\gamma}A^*)}{\partial I} - \frac{\mathcal{F}(S^*,A^*)+\mathcal{G}(S^*,I^*)}{A^*} \\
&= -\frac{\zeta_1}{\zeta_2}\frac{\partial \mathcal{F}(S^*,A^*)}{\partial S} - \frac{\zeta_1}{\zeta_2}\frac{\partial \mathcal{G}(S^*,\frac{\phi}{\mu+\gamma}A^*)}{\partial S} + \frac{1}{A^*}\left(A^*\frac{\partial \mathcal{F}(S^*,A^*)}{\partial A} - \mathcal{F}(S^*,A^*)\right) \\
&\quad + \frac{\phi I^*}{\mu+\gamma}\left(I^*\frac{\partial \mathcal{G}(S^*,I^*)}{\partial I} - \mathcal{G}(S^*,I^*)\right) < 0.
\end{aligned}$$

Thus, $\mathcal{H}$ is strictly decreasing at every zero. So, when $R_0 > 1$, the system (1.1) has a unique endemic equilibrium A^*. Otherwise, if there exists another endemic equilibrium $\hat{A}$ other than A^*, then $\mathcal{H}^{'}(\hat{A}) \geq 0$, which is a contradiction. Also, when $R_0 < 1$, we claim that system (1.1) has no endemic equilibrium. To this end, we know that $\mathcal{H}^{'}(0) < 0$ when $R_0 < 1$. Hence, $\mathcal{H}(A) < 0$ for sufficiently A. Finally, we conclude that $\mathcal{H}^{'}(A)$ is negative at any positive equilibrium. Nevertheless, in order for $\mathcal{H}$ to increase to 0 at a point $\hat{A}$, we should get $\mathcal{H}^{'}(\hat{A}) \geq 0$, which is a contradiction. □

Now, we study the local stability of the equilibrium points of the system (1.1).

Theorem 2.3. *If $R_0 < 1$, the disease-free equilibrium Θ_0 of the system (1.1) is locally asymptotically stable, while Θ_0 is an unstable if $R_0 > 1$.*

Proof. The Jacobian matrix of the system (1.1) around Θ_0 is

$$J|_{\Theta_0} = \begin{pmatrix}
-\mu & -\frac{\partial \mathcal{F}(\frac{\lambda}{\mu},0)}{\partial A} & -\frac{\partial \mathcal{G}(\frac{\lambda}{\mu},0)}{\partial I} & \tau \\
0 & \frac{\partial \mathcal{F}(\frac{\lambda}{\mu},0)}{\partial A} - (\mu+\phi) & \frac{\partial \mathcal{G}(\frac{\lambda}{\mu},0)}{\partial I} & 0 \\
0 & \phi & -(\mu+\gamma) & 0 \\
0 & 0 & \gamma & -(\tau+\mu)
\end{pmatrix}.$$

The characteristic equation of $J|_{\Theta_0}$ is as follows:

$$\mathcal{P}(r) := (-\mu-r)(-(\tau+\mu)-r)\det\begin{pmatrix}
\frac{\partial \mathcal{F}(\frac{\lambda}{\mu},0)}{\partial A} - (\mu+\phi) - r & \frac{\partial \mathcal{G}(\frac{\lambda}{\mu},0)}{\partial I} \\
\phi & -(\mu+\gamma)-r
\end{pmatrix}.$$

Clearly, $\lambda_1 = -\mu$ and $\lambda_2 = -(\tau+\mu)$ are two eigenvalues of $J|_{\Theta_0}$. To calculate other eigenvalues, we consider the following matrix

$$P_{\Theta_0} = \begin{pmatrix}
\frac{\partial \mathcal{F}(\frac{\lambda}{\mu},0)}{\partial A} - (\mu+\phi) & \frac{\partial \mathcal{G}(\frac{\lambda}{\mu},0)}{\partial I} \\
\phi & -(\mu+\gamma)
\end{pmatrix},$$

and so by (H4),

$$\operatorname{trace}(P_{\Theta_0}) = \frac{\partial \mathcal{F}(\frac{\lambda}{\mu},0)}{\partial A} - (\mu+\phi) - (\mu+\gamma) < 0,$$

and by $R_0 < 1$,

$$\det(P_{\Theta_0}) = (\mu+\phi)(\mu+\gamma)[1-R_0] < 0.$$

If $R_0 < 1$, then the eigenvalues of P_{Θ_0} have a negative real part, and then Θ_0 is locally asymptotically stable. □

Theorem 2.4. *The endemic equilibrium point Θ^* of the system (1.1) is locally asymptotically stable if $R_0 > 1$.*

Proof. The Jacobian matrix of the system (1.1) around Θ^* is

$$J|_{\Theta^*} = \begin{pmatrix} -\mu - \frac{\partial \mathcal{F}(S^*,A^*)}{\partial S} - \frac{\partial \mathcal{G}(S^*,I^*)}{\partial S} & -\frac{\partial \mathcal{F}(S^*,A^*)}{\partial A} & -\frac{\partial \mathcal{G}(S^*,I^*)}{\partial I} & \tau \\ \frac{\partial \mathcal{F}(S^*,A^*)}{\partial S} + \frac{\partial \mathcal{G}(S^*,I^*)}{\partial S} & \frac{\partial \mathcal{F}(S^*,A^*)}{\partial A} - (\mu+\phi) & \frac{\partial \mathcal{G}(S^*,I^*)}{\partial I} & 0 \\ 0 & \phi & -(\mu+\gamma) & 0 \\ 0 & 0 & \gamma & -(\tau+\mu) \end{pmatrix}.$$

Clearly, the characteristics equation of $J|_{\Theta^*}$ is

$$r^4 + \eta_1 r^3 + \eta_2 r^2 + \eta_3 r + \eta_4 = 0, \tag{2.8}$$

where

$$\begin{aligned}
\eta_1 &= \mu + \frac{\partial \mathcal{F}(S^*,A^*)}{\partial S} + \frac{\partial \mathcal{G}(S^*,I^*)}{\partial S} - \frac{\partial \mathcal{F}(S^*,A^*)}{\partial A} + (\mu+\phi) + (\mu+\gamma) + (\tau+\mu),\\
\eta_2 &= \left(\mu + \frac{\partial \mathcal{F}(S^*,A^*)}{\partial S} + \frac{\partial \mathcal{G}(S^*,I^*)}{\partial S}\right)\left((\mu+\phi) + (\mu+\gamma) - \frac{\partial \mathcal{F}(S^*,A^*)}{\partial A}\right)\\
&\quad + (\mu+\gamma)(\tau+\mu) + (\tau+\mu)\left(\mu + \frac{\partial \mathcal{F}(S^*,A^*)}{\partial S} + \frac{\partial \mathcal{G}(S^*,I^*)}{\partial S}\right)\\
&\quad + (\mu+\gamma+\tau+\mu)\left((\mu+\phi) - \frac{\partial \mathcal{F}(S^*,A^*)}{\partial A}\right) - \phi\frac{\mathcal{G}(S^*,I^*)}{\partial I}\\
&\quad + \frac{\partial \mathcal{F}(S^*,A^*)}{\partial A}\left(\frac{\partial \mathcal{F}(S^*,A^*)}{\partial S} + \frac{\partial \mathcal{G}(S^*,I^*)}{\partial S}\right),\\
\eta_3 &= \left(\mu + \frac{\partial \mathcal{F}(S^*,A^*)}{\partial S} + \frac{\partial \mathcal{G}(S^*,I^*)}{\partial S}\right)\left((\mu+\phi) - \frac{\partial \mathcal{F}(S^*,A^*)}{\partial A}\right)((\mu+\gamma) + (\tau+\mu))\\
&\quad + (\mu+\gamma)(\tau+\mu)\left[\mu + \frac{\partial \mathcal{F}(S^*,A^*)}{\partial S} + \frac{\partial \mathcal{G}(S^*,I^*)}{\partial S} + (\mu+\phi) - \frac{\partial \mathcal{F}(S^*,A^*)}{\partial A}\right]\\
&\quad - \phi\frac{\mathcal{G}(S^*,I^*)}{\partial I}(2\mu+\tau) + \frac{\partial \mathcal{F}(S^*,A^*)}{\partial E}\left(\frac{\partial \mathcal{F}(S^*,A^*)}{\partial S} + \frac{\partial \mathcal{G}(S^*,I^*)}{\partial S}\right)(2\mu+\gamma+\tau),\\
\eta_4 &= -\left(\frac{\partial \mathcal{F}(S^*,A^*)}{\partial S} + \frac{\partial \mathcal{G}(S^*,I^*)}{\partial S}\right)\left[\phi(\tau+\mu)\frac{\mathcal{G}(S^*,I^*)}{\partial I} + \gamma\tau\phi\right]\\
&\quad - \left(\mu + \frac{\partial \mathcal{F}(S^*,A^*)}{\partial S} + \frac{\partial \mathcal{G}(S^*,I^*)}{\partial S}\right)\left((\mu+\phi) - \frac{\partial \mathcal{F}(S^*,A^*)}{\partial A}\right)(\mu+\gamma)(\tau+\mu).
\end{aligned}$$

By (H3) and (H4), it follows that $\eta_i > 0, i = 1,2,3,4$, and $\eta_1\eta_2\eta_3 > \eta_1^2\eta_4 + \eta_3^2 > 0$. So, by the Routh-Hurwitz criterion Θ^* is locally asymptotically stable if $R_0 > 1$. □

Theorem 2.5. *If $R_0 \le 1$, then the disease-free equilibrium Θ_0 of the system (1.1) is globally asymptotically stable. If $R_0 > 1$, then the endemic equilibrium Θ^* of the system (1.1) is globally asymptotically stable.*

Proof. By Proposition 2.2 of [18], the solution $\xi(t) = (S(t), A(t), I(t), R(t))$ of (1.1) has the limit as $t \to +\infty$. Set $\lim_{t\to\infty}\xi(t) = (S_\infty, A_\infty, I_\infty, R_\infty)$. From (H3) and Lemma 2.1, we have that $\frac{d\xi}{dt}$ is uniformly bounded, and so by

continuity of $\mathcal{F}$ and $\mathcal{G}$, we deduce that $\frac{d\xi}{dt}$ is uniformly continuous. So, using the Barbalat's Lemma [5], one can get $\lim_{t\to\infty}\dot{\xi}(t)=(0,0,0,0)$. By system (1.1), we have

$$\begin{cases}\lambda-\mathcal{F}(S_\infty,A_\infty)-\mathcal{G}(S_\infty,I_\infty)-\mu S_\infty+\tau R_\infty=0,\\ \mathcal{F}(S_\infty,A_\infty)+\mathcal{G}(S_\infty,I_\infty)-(\mu+\phi)A_\infty=0,\\ \phi A_\infty-(\mu+\gamma)I_\infty=0,\\ \gamma I_\infty-(\mu+\tau)R_\infty=0,\end{cases}$$

and so $(S_\infty,A_\infty,I_\infty,R_\infty)$ is an equilibrium point of the system (1.1). Hence, in view of Theorem 2.2, we get $\lim_{t\to\infty}\xi(t)=\Theta^*$ or $\lim_{t\to\infty}\xi(t)=\Theta_0$. If $R_0<1$, then Θ^* does not exist, thus $\lim_{t\to\infty}\xi(t)=\Theta_0$. If $R_0=1$, $\Theta^*=\Theta_0$, then $\lim_{t\to\infty}\xi(t)=\Theta_0$. If $R_0>1$, by Theorem 2.3, Θ_0 is unstable, so we conclude $\lim_{t\to\infty}\xi(t)=\Theta^*$. □

Theorem 2.6. *The system (1.1) does not have nontrivial periodic orbits.*

Proof. Using the vector notation $X=(S,A,I,R)^T$, the model (1.1) can be formulated as $(\frac{dX}{dt})=(f_1,f_2,f_3,f_4)^T=(\mathbf{f})$. Then, we have

$$\nabla\cdot\mathbf{f}=-\frac{\partial\mathcal{F}(S,A)}{\partial S}-\frac{\partial\mathcal{G}(S,I)}{\partial I}-\mu+\underbrace{\frac{\partial\mathcal{F}(S,A)}{\partial A}}_{<0\text{ (by (H4))}}-(\mu+\phi)-(\mu+\gamma)-(\tau+\mu)<0.$$

Therefore, according to Dulac's criterion [34, Theorem 4.1.2], we have the conclusion. □

3. Numerical simulations of the SAIR model

This section is devoted to the numerical simulation of stability of the disease-free and endemic equilibriums. This will also confirm our theoretical findings. We will use the fourth order Runge-Kutta (RK4) numerical scheme in order to solve our mathematical model. For a broader view of the infection dynamics, different incidence functions will be considered. Indeed, numerical tests will be performed for four different cases:

(i) the first is to study the system (1.1) under the simplest two-bilinear incidence functions $\mathcal{F}(S,A)=\alpha_1SA$ and $\mathcal{G}(S,I)=\alpha_2SI$;

(ii) Beddington-DeAngelis incidence functions, $\mathcal{F}(S,A)=\dfrac{\alpha_1S}{1+\sigma_1S+\sigma_2A}$ and $\mathcal{G}(S,I)=\dfrac{\alpha_2S}{1+\sigma_3S+\sigma_4I}$;

(iii) Crowley-Martin functions, $\mathcal{F}(S,A)=\dfrac{\alpha_1S}{1+\xi_1S+\xi_2A+\xi_1\xi_2SA}$ and $\mathcal{G}(S,I)=\dfrac{\alpha_2S}{1+\xi_3S+\xi_4I+\xi_3\xi_4SI}$;

(iv) non-monotonic incidence function $\mathcal{F}(S,A)=\frac{\alpha_1SA}{1+\kappa_1A^2}$ and $\mathcal{G}(S,I)=\frac{\alpha_2SI}{1+\kappa_2I^2}$.

For each numerical test, we will take the fixed initial conditions: $S(0)=4$, $A(0)=2$, $I(0)=1$, and $R(0)=0$. The formula (2.3) for the basic reproduction number is written in its general form in terms of two incidence rates of general form. For our numerical simulation, the basic reproduction number for the two-bilinear case is equal to $R_0^{\mathcal{B}L}=\frac{\alpha_1\lambda}{\mu^2+\mu\phi}+\frac{\alpha_2\lambda\phi}{(\mu+\gamma)(\mu^2+\mu\phi)}$. For two-incidence functions of Beddington-DeAngelis forms, the reproduction number is $R_0^{\mathcal{B}D}=\dfrac{\alpha_1\lambda}{(\mu+\phi)(\mu+\sigma_1\lambda)}+\dfrac{\alpha_2\lambda\phi}{(\mu+\phi)(\mu+\gamma)(\mu+\sigma_3\lambda)}$. For the incidence rates of Crowley-Martin and non-monotonic forms, the basic reproduction numbers are $R_0^{\mathcal{C}M}=\frac{\alpha_1\lambda}{(\mu+\phi)(\mu+\xi_1\lambda)}+\frac{\alpha_2\lambda\phi}{(\mu+\phi)(\mu+\gamma)(\mu+\xi_3\lambda)}$ and $R_0^{\mathcal{N}M}=\frac{\alpha_1\lambda}{\mu^2+\mu\phi}+\frac{\alpha_2\lambda\phi}{(\mu+\gamma)(\mu^2+\mu\phi)}$. For the four cases under investigation, each basic reproduction number is written as a summation of two numbers: the first reflects the effect of the first incidence effect while the second represents the effect, of the second incidence function. Our RK4 approach numerical experiments were conducted with the aid of MATLAB software.

3.1. Disease-free equilibrium stability.

In order to illustrate the stability of the disease-free equilibrium, we will chose the following parameters $\lambda=1$, $\mu=0.2$, $\tau=0.05$, $\phi=0.5$, $\gamma=0.15$, $\alpha_1=0.05$, $\alpha_2=0.01$, $\sigma_1=0.4$, $\sigma_2=0.85$, $\sigma_3=4.5$, $\sigma_4=5.8$, $\xi_1=2.5$, $\xi_2=3$, $\xi_3=6.5$, $\xi_4=5$, $\kappa_1=2.5$, and $\kappa_2=3$. Within these chosen parameters, Figure 2 shows the behaviour of the dynamics for our SAIR infection model. The figure shows that the susceptible reach their maximum value for the four different incidence cases; while the other compartments representing the asymptomatic, symptomatic, and recovered individuals vanish. Precisely, we observe the convergence of the curves

toward the free-disease equlibrium $\Theta_0 = (5, 0, 0, 0)$. The basic reproduction numbers for the four incidence cases are as follows: $R_0^{\mathcal{B}L} = 0.459$ for the bilinear incidence functions, $R_0^{\mathcal{B}D} = 0.123$ for Beddington-DeAngelis case, $R_0^{\mathcal{C}M} = 0.029$ for Crowley-Martin incidences and $R_0^{\mathcal{N}M} = 0.459$ for non-monotonic incidence functions. For the four different cases the basic reproduction number is less than unity, which confirms our theoretical results concerning the stability of the disease-free equilibrium.

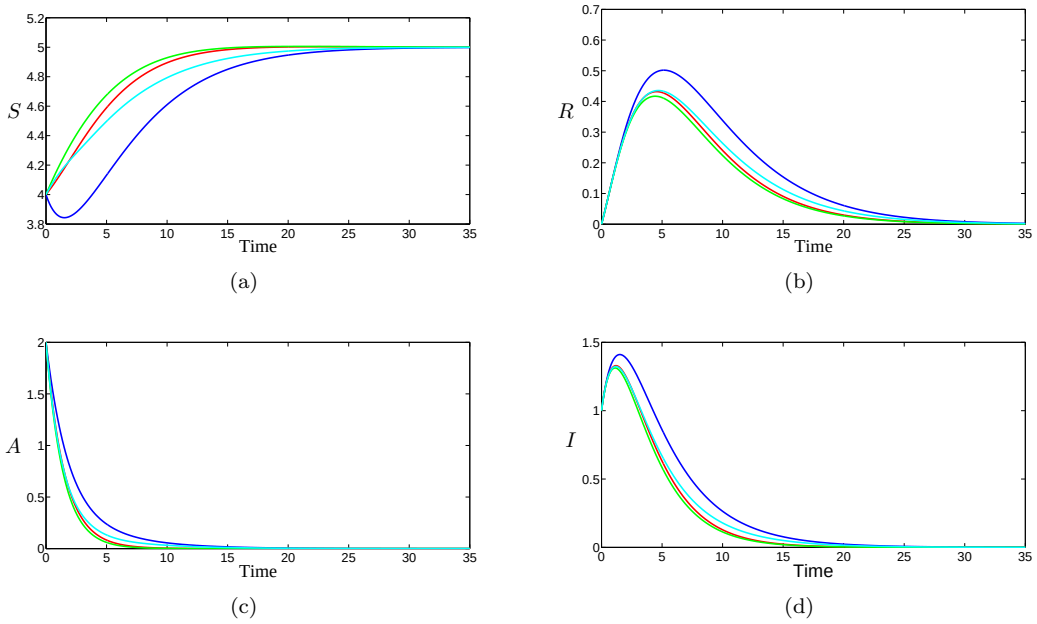

FIGURE 2. The time evolution of susceptible, (a) the recovered, (b) the asymptomatic infected, (c) the symptomatic infected individuals, (d) illustrates the stability of the free equilibrium Θ_0. The bilinear incidence functions (blue), Beddington-DeAngelis incidence functions (red), Crowley-Martin incidence functions (green) and the non-monotone incidence functions (cyan color).

3.2. **Endemic equilibrium stability.** To illustrating the stability of the endemic equilibrium, we take parameters $\lambda = 1$, $\mu = 0.2$, $\tau = 0.05$, $\phi = 0.5$, $\gamma = 0.15$, $\alpha_1 = 0.5$, $\alpha_2 = 0.1$, $\sigma_1 = 0.4$, $\sigma_2 = 0.85$, $\sigma_3 = 4.5$, $\sigma_4 = 5.8$, $\xi_1 = 0.5$, $\xi_2 = 3$, $\xi_3 = 0.5$, $\xi_4 = 5$, $\kappa_1 = 2.5$, and $\kappa_2 = 3$. With these chosen parameters, Figure 3 depicts the behaviour of the dynamics for our SAIR infection model. The figure demonstrates that the susceptible, the asymptomatic, symptomatic and recovered individuals stay at a strictly positive level which reveal that the infection persists. In precise terms, the curves converge of the curves toward the endemic equilibrium $\Theta^*_{\mathcal{B}L} = (1.088, 1.190, 1.700, 1.021)$ when both the incidence functions take the bilinear forms, $\Theta^*_{\mathcal{B}D} = (3.823, 0.358, 0.511, 0.308)$ when the incidences are under Beddington-DeAngelis formulation, $\Theta^*_{\mathcal{C}M} = (4.652, 0.104, 0.150, 0.094)$ for the incidence rates of Crowley-Martin forms and finally towards the endemic equilibrium $\Theta^*_{\mathcal{N}M} = (2.659, 0.701, 1.002, 0.602)$ for non-monotonic incidence rates. It is easy to check that the components of each endemic case verify the formulas (2.5)-(2.7). Moreover, calculating the basic reproduction number for each case are $R_0^{\mathcal{B}L} = 4.591$ for the bilinear incidence functions, $R_0^{\mathcal{B}D} = 1.233$ for Beddington-DeAngelis case, $R_0^{\mathcal{C}M} = 1.311$ for Crowley-Martin incidences and $R_0^{\mathcal{N}M} = 4.591$ for non-monotonic incidence functions. For the four different cases the basic reproduction number is greater than unity confirming our theoretical results concerning the stability of the endemic equilibrium.

3.3. **Temporary immunity effect.** In this subsection, we will discuss the effect of the temporary immunity on the infection. Indeed, we consider the same values as in the previous subsection, except for the value of the temporary

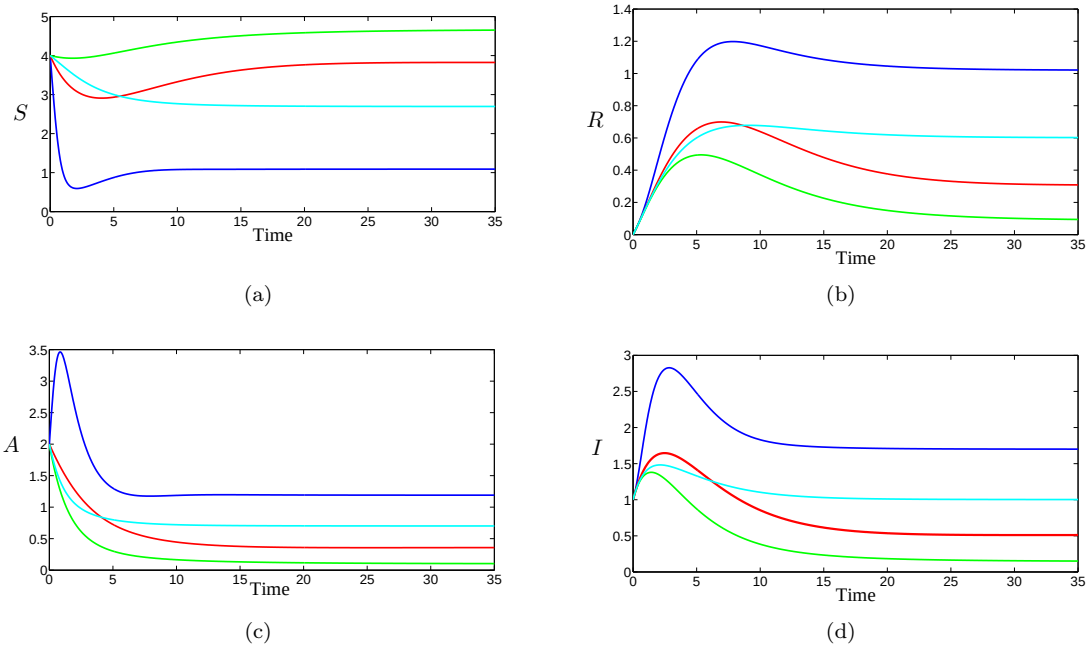

FIGURE 3. The time evolution of susceptible, (a) the recovered, (b) the asymptomatic infected, (c) the symptomatic infected individuals, (d) illustrates the stability of the free equilibrium Θ^*. The bilinear incidence functions (blue), Beddington-DeAngelis incidence functions (red), Crowley-Martin incidence functions (green) and the non-monotone incidence functions (cyan color).

immunity τ that we will change three times. In fact, we will choose the following parameters $\lambda = 1$, $\mu = 0.2$, $\phi = 0.5$, $\gamma = 0.15$, $\alpha_1 = 0.5$, $\alpha_2 = 0.1$, and three values of the value of τ as indicated in Figure 4. For the three values of immunity, we only consider the bilinear incidence rates. The figure clearly shows the effect of the temporary immunity on both the asymptomatic and symptomatic infected populations. Notice that the increase in the temporary immunity rate increases the infected population, that is, when a higher rate of the recovered loses its immunity, the infected population becomes larger. On the contrary, when the temporary immunity rate is increased, the susceptible and the recovered populations decrease (not shown). This result demonstrates the significance of temporary immunity on the infection spread, which means that a good vaccine can lead to an efficient immunity to the population and maximizes the immunity duration and makes the entire population safer for a long period.

4. Conclusion

In this paper, we have studied the dynamics of a SAIR mathematical model that describes the interaction between susceptible, asymptomatic, symptomatic, and recovered individuals. Two general incidence functions are taken into account: the first describes the infection caused by asymptomatic persons, while the second stands for the infection generated by the symptomatic ones. In addition, introducing temporary immunity in our model makes it more realistic. The basic reproduction number is found depending on the general incidence functions. It was demonstrated that the disease-free equilibrium exists when the basic reproduction number is less than one. On the other hand, when this number exceeds unity, the endemic equilibrium exists. The local and global asymptotic stability for each equilibrium is proved using the basic reproduction number. The numerical simulations are performed for different cases of the incidence rates, such as bilinear incidence functions, Beddington-DeAngelis incidences, Crowley-Martin functions, and non-monotonic rates. The numerical simulation confirms our theoretical findings for each case.

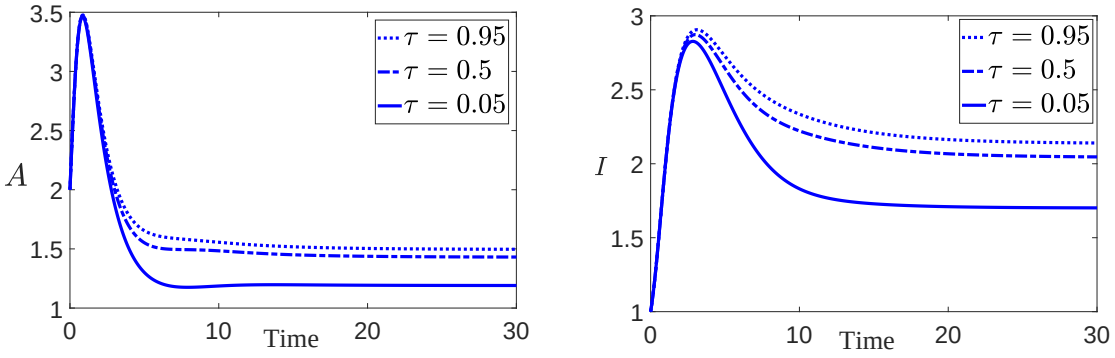

(a) (b)

FIGURE 4. The time evolution of the asymptomatic infected, (a) the symptomatic infected individuals, (b) for different values of the temporary immunity rate.

CONFLICT OF INTEREST

The authors declare that they have no conflict of interest.

ACKNOWLEDGMENT

The authors would like to thank the referees for their suggestions and helpful comments which improved the presentation of the original manuscript.

REFERENCES

[1] R. T. Alqahtani, *Mathematical model of SIR epidemic system (COVID-19) with fractional derivative: stability and numerical analysis*, Advances in Difference Equations, *2021*(1) (2021), 1–16.
[2] L. J. S. Allen, *Some discrete-time SI, SIR, and SIS epidemic models*, Mathematical Biosciences, *124* (1994), 83–105.
[3] L. J. S. Allen, Y. Lou, and A. L. Nevai, *Spatial patterns in a discrete-time SIS patch model*, Journal of Mathematical Biology, *58* (2009), 339–375.
[4] S. Ansumali, S. Kaushal, A. Kumar, M. K. Prakash, and M. Vidyasagar, *Modelling a pandemic with asymptomatic patients, impact of lockdown and herd immunity, with applications to SARS-CoV-2*, Annual Reviews in Control, *50* (22020), 432–447.
[5] I. Barbâlat, *Systèmes d'ǫuations différentielles d'oscillations non Linéaires*, Revue roumaine de mathématiques pures et appliquées, *4* (1959), 267–270.
[6] J. R. Beddington, *Mutual interference between parasites or predators and its effect on searching efficiency*, Journal of Animal Ecology, *44* (1975), 331–341.
[7] M. Bisiacco, G. Pillonetto, and C. Cobelli, *Closed-form expressions and nonparametric estimation of COVID-19 infection rate*, Automatica, *140* (2022), 110265.
[8] O. N. Bjrnstad, B. F. Finkenstaedt, and B. T. Greenfell, *Dynamics of measles epidemics: estimating scaling of transmission rates using a time series SIR model*, Ecological Monographs, *72* (2002), 169–184.
[9] R. S. Cantrell and C. Cosner, *On the dynamics of predator-prey models with the Beddington-DeAngelis functional response*, Journal of Mathematical Analysis and Applications, *257* (2001), 206–222.
[10] P. H. Crowley and E. K. Martin, *Functional responses and interference within and between year classes of a dragonfly population*, Journal of the North American Benthological Society, *8* (1989), 211–221.
[11] R. Casagrandi, L. Bolzoni, S. A. Levin, and V. Andreasen, *The SIRC model for influenza* Mathematical Biosciences, *200* (2006), 152–169.

[12] M. Das and G. P. Samanta, *Optimal control of fractional order COVID-19 epidemic spreading in Japan and India 2020*, Biophysical Reviews and Letters, *15*(04) (2020), 207–236.
[13] D. L. DeAngelis, R. A. Goldstein, and R. V. O'Neill, *A model for tropic interaction*, Ecology, *56* (1975), 881–892.
[14] K. Goel Nilam, *A nonlinear SAIR epidemic model: Effect of awareness class, nonlinear incidences, saturated treatment and time delay* Ricerche di Matematica, *2022* (2022), 1–35.
[15] M. Grunnill, *An exploration of the role of asymptomatic infections in the epidemiology of dengue viruses through susceptible, asymptomatic, infected and recovered (SAIR) models*, Journal of theoretical biology, *439* (2020), 106442.
[16] J. K. Hale, S. M. V. Lunel, and L. S. Verduyn, *Introduction to functional differential equations*, Springer, New York, *99* (1993).
[17] W. Hamer, *The milroy lectures on epidemic disease in england the evidence of variability and persistence of type*, Lancet 1, (1906), 733–739.
[18] K. Hattaf, N. Yousfi, and A. Tridane, *Mathematical analysis of a virus dynamics model with general incidence rate and cure rate*, Nonlinear Anal. (RWA), *13*(4) (2012), 1866–1872.
[19] J. Jiao, Z. Liu, and S. Cai, *Dynamics of an SEIR model with infectivity in incubation period and homestead-isolation on the susceptible*, Applied Mathematics Letters, *107* (2020), 106442.
[20] W. Kermack and A. McKendrick, *Contributions to the mathematical theory of epidemics-I*, Proceedings of the Royal Society A, *115* (1927), 700–721.
[21] M. A. Khan, Y. Khan, and S. Islam, *Complex dynamics of an SEIR epidemic model with saturated incidence rate and treatment*, Physica A, *493* (2018), 210–227.
[22] O. Khyar and K. Allali, *Global dynamics of a multi-strain SEIR epidemic model with general incidence rates: application to COVID-19 pandemic*, Nonlinear Dynamics, *102* (2020), 489-509.
[23] O. Khyar and K. Allali, *Dynamic Analysis of a three-Strain COVID-19 SEIR epidemic model with general incidence rates*, Advances in Nonlinear Dynamics, *2022* (2022), 49–59.
[24] X. Zhang, Z. Li, and L. Gao, *Stability analysis of a SAIR epidemic model on scale-free community networks*, Mathematical Biosciences and Engineering, *21*(3) (2024), 4648–4668.
[25] X. Liu and L. Yang, *Stability analysis of an SEIQV epidemic model with saturated incidence rate*, Nonlinear Analysis: Real World Applications, *13* (2012), 2671–2679.
[26] X. Q. Liu, S. M. Zhong, B. D. Tian, and F. X. Zheng, *Asymptotic properties of a stochastic predator-prey model with Crowley-Martin functional response*, Journal of Applied Mathematics and Computing, *43* (2013), 479–490.
[27] L. H. A. Monteiro, *An epidemiological model for SARS-CoV-2*, Ecological Complexity, *43* (2020), 100836.
[28] N. Ozalp and E. Demirrci, *A fractional order SEIR model with vertical transmission*, Mathematical and Computer Modelling, *54*(12) (2011), 1–6.
[29] I. Nesteruk, *Detections and SIR simulations of the COVID-19 pandemic waves in Ukraine*, Computational and Mathematical Biophysics, *9* (2021), 46–65.
[30] R. Ross, *The prevention of malaria*, New York: EP Dutton and Company, (1910).
[31] P. Samui, J. Mondal, B. Ahmad, and A. N. Chatterjee, *Clinical effects of 2-DG drug restraining SARS-CoV-2 infection: A fractional order optimal control study*, J. Biological Physics, *48* (2022), 415–438.
[32] T. Sitthiwirattham, A. Zeb, S. Chasreechai, Z. Eskandari, M. Tilioua, and S. Djilali, *Analysis of a discrete mathematical COVID-19 model*, Results in Physics, *28* (2021), 104668.
[33] P. Van den Driessche and J. Watmough, *Reproduction numbers and sub-threshold endmic equlibria for compartmental models of diesease transmission*, Mathematical Biosciences, *180* (2002), 29–48.
[34] S. Wiggins, *Introduction to applied nonlinear dynamical systems and chaos*, Springer, (2003).
[35] L. Ying and T. Xiaoqing, *COVID-19: Is it safe now? Study of asymptomatic infection spread and quantity risk based on SAIR model*, Chaos Solitons Fractals, *6* (2021), 100060.
[36] X. Zhou and J. Cui, *Global stability of the viral dynamics with Crowley-Martin functional response*, Bulletin of the Korean Mathematical Society, *48* (2011), 555–574.
[37] Y. Zhao and D. Jiang, *The threshold of a stochastic SIRS epidemic model with saturated incidence*, Applied Mathematics Letters, *34* (2014), 90–93.